

# Peculiar velocities of galaxy clusters: a comparison with the linear theory

Mirt Gramann and Ivan Suhhonenko

*Tartu Observatory, Tõravere 61602, Estonia*

3 September 2018

## ABSTRACT

We investigate peculiar velocities predicted for clusters in Lambda cold dark matter ( $\Lambda$ CDM) models assuming that the initial density fluctuation field is Gaussian. To study the non-linear regime, we use N-body simulations. We investigate the rms velocity and the probability distribution function of cluster peculiar velocities for different cluster masses. To identify clusters in the simulation we use two methods: the standard friends-of-friends (FOF) method and the method, where the clusters are defined as maxima of a smoothed density field (DMAX). The density field is smoothed with a top-hat window, using the smoothing radii  $R_s = 1.5h^{-1}$  Mpc and  $R_s = 1.0h^{-1}$  Mpc. The peculiar velocity of the DMAX clusters is defined to be the mean peculiar velocity of matter within a sphere of the radius  $R_s$ . We find that the rms velocity of the FOF clusters decreases as the cluster mass increases. The rms velocity of the DMAX clusters is almost independent of the cluster mass and is well approximated by the linear rms peculiar velocity smoothed at the radius  $R = R_s$ . The velocity distribution function of the DMAX clusters is similar to a Gaussian.

**Key words:** galaxies: clusters: general – cosmology: theory – dark matter – large-scale structure of Universe.

## 1 INTRODUCTION

One of the interesting problems in cosmology is the evolution of the large-scale peculiar velocity field in the Universe. The evolution of the large-scale velocity field has been studied in a number of papers (see, e.g., Davis et al. 1985; Kofman et al. 1994; Brainerd & Villumsen 1994; Gramann et al. 1995; Jenkins et al. 1998; Juszkiewicz, Springel & Durrer 1999; Colin, Klypin & Kravtsov 2000; Gramann & Suhhonenko 2002; Ciecielag et al. 2003). The linear rms peculiar velocity on a given scale  $R$  can be expressed as

$$\sigma_v(R) = H_0 f \sigma_{-1}(R), \quad (1)$$

where  $H_0$  is the Hubble constant and  $f$  is the dimensionless growth rate, which is related to the cosmological matter density parameter,  $\Omega_m$ , and the cosmological constant,  $\Omega_\Lambda$ , by

$$f(\Omega_m, \Omega_\Lambda) \simeq \Omega_m^{0.6} + \frac{\Omega_\Lambda}{70} \left(1 + \frac{\Omega_m}{2}\right) \quad (2)$$

(Lahav et al. 1991). The spectral moments  $\sigma_j(R)$  are defined for any integer  $j$  by

$$\sigma_j^2(R) = \frac{1}{2\pi^2} \int P(k) W^2(kR) k^{2j+2} dk, \quad (3)$$

where  $P(k)$  is the power spectrum of density fluctuations and  $W(kR)$  is a Fourier transform of the smoothing window.

For the top-hat window in real space that we will use in this paper,  $W(x) = (3/x^3)[\sin(x) - x \cos(x)]$ . Notice that the predicted rms peculiar velocity depends both on cosmology and on the shape of the power spectrum.

Jenkins et al. (1998) used a N-body simulation to investigate the rms peculiar velocity of the dark matter smoothed on the scales  $R = 10 - 80h^{-1}$  Mpc. They compared the results with the linear approximation (1) and found that on scales above  $20h^{-1}$  Mpc, the linear theory prediction agrees very well with the simulation. Kofman et al. (1994) and Ciecielag et al. (2003) studied the evolution of the peculiar velocity one-point distribution function, beginning with Gaussian initial fluctuations. They showed that on mildly non-linear scales ( $4 - 10h^{-1}$  Mpc, Gaussian smoothing) the distribution of the Cartesian components of the peculiar velocity field is well approximated by a Gaussian. On smaller scales the velocity distribution of dark matter becomes non-Gaussian due to the motions of matter within dense systems (see e.g. Sheth & Diaferio (2001) for the discussion of the velocity distribution of dark matter particles in different cosmological models).

Important information for the large-scale velocity field is provided by peculiar velocities of galaxy clusters. The evolution of peculiar velocities of clusters in different cosmological models has been examined in several papers (e.g. Bahcall, Gramann & Cen 1994; Croft & Efstathiou 1994;

Moscardini et al. 1996; Suhhonenko & Gramann 1999; Colberg et al. 2000; Sheth & Diaferio 2001; Suhhonenko & Gramann 2003; Hamana et al. 2003). Clusters represent high-density maxima in the dark matter density field. Bardeen et al. (1986) studied the peculiar velocity distribution for peaks of a Gaussian density field. They showed that the velocity distribution function for peaks is also Gaussian, with the rms peculiar velocity

$$\sigma_p(R) = \sigma_v(R) \sqrt{1 - \sigma_0^4 / \sigma_1^2 \sigma_{-1}^2}. \quad (4)$$

Peaks have lower peculiar velocities than field points. The reason for this difference is the fact that the velocity field is correlated with the density gradient field. However, at radii  $R \sim 1 - 5h^{-1}$  Mpc, the difference between  $\sigma_v(R)$  and  $\sigma_p(R)$  is small in standard cosmological models. For example, in the flat  $\Omega_m = 0.3$   $\Lambda$ CDM model, it is about 3 per cent at the radius  $R = 1.5h^{-1}$  Mpc. Gramann et al. (1995) studied the large-scale velocity and potential maps of clusters and of the matter using N-body simulations. They found that the large-scale velocity and potential fields are recovered remarkably well by using the velocities of clusters,

In this paper we study peculiar velocities of clusters in a  $\Lambda$ CDM model. We use the N-body simulation carried out by the Virgo Consortium for the flat  $\Lambda$ CDM model with the density parameter  $\Omega_m = 0.3$  (Jenkins et al. 1998). To identify clusters in the simulation we use two methods: (1) the standard friends-of-friends (FOF) method and (2) the method, where the clusters are defined as the maxima of the smoothed density field (DMAX). We use a top-hat window with the smoothing radii  $R_s = 1.5h^{-1}$  Mpc and  $R_s = 1h^{-1}$  Mpc. The velocity and the mass of FOF clusters are defined to be as mean velocity and the total mass of all the particles in the cluster. To determine the mass and velocity of DMAX clusters, we use the same smoothing as for the density field. We study the rms velocity of clusters for different cluster masses. The rms peculiar velocity of clusters was studied also by Suhhonenko & Gramann (2003). They used a somewhat different DMAX method. The densities and peculiar velocities of clusters were determined using the cloud-in-cell (CIC) scheme. In this paper we use a top-hat window, which allows us to simply calculate cluster masses.

We compare the rms velocity of clusters in the simulation with the linear approximation (4). What window function,  $W(kR)$ , and smoothing length,  $R$ , for the spectral moments in the equation (4) are appropriate for cluster velocities? Different studies have used different window functions and smoothing lengths. Croft & Efstathiou (1994) and Bahcall, Gramann & Cen (1994) used Gaussian smoothing with a radius  $R = 3h^{-1}$  Mpc. Suhhonenko & Gramann (1999) adopted top-hat smoothing with a radius  $R = 1.5h^{-1}$  Mpc. To compare model predictions with the observed peculiar velocities of galaxy clusters, Borgani et al. (2000) used Gaussian smoothing with a radius  $R = 1.5h^{-1}$  Mpc. Colberg et al. (2000) and Sheth & Diaferio (2001) connected the smoothing length  $R$  in the equation (4) with the cluster mass  $M$ . They studied the rms peculiar velocity,  $\sigma_p(R)$ , at the linear radius  $R = R_L(M)$ , where the linear radius  $R_L$  is defined as  $M = 4\pi/3\rho_b R_L^3$  (here  $\rho_b$  is the mean background density). Similar approach was used recently by Hamana et al. (2003).

The velocity of DMAX clusters is determined as the mean velocity of matter within a sphere of radius  $R_s = 1.5h^{-1}$  Mpc (or  $R_s = 1h^{-1}$  Mpc). In other words, we use

top-hat smoothing with a radius  $R_s$ . For this reason, we adopt also the top-hat window function and the smoothing radius  $R = R_s$  in the equation (4). We consider also the rms peculiar velocity,  $\sigma_p$ , at the radius  $R = R_L(M)$ .

The sizes of FOF clusters are not fixed. If we use the FOF method, the mean size of high-mass clusters is larger than the mean size of low-mass clusters. Therefore, it is not possible to connect the rms velocities of FOF clusters with a single radius  $R = R_s$ . We can use the approximation  $R = R_L(M)$ . Note that for the DMAX clusters, the ratio  $R_L^3/R_s^3 = \rho/\rho_b$ , where  $\rho$  is the mean cluster density within a sphere of radius  $R_s$ . For  $\rho/\rho_b \approx 200$ , the ratio  $R_L/R_s \approx 6$ .

We also investigate the velocity distribution function of clusters. We examine the distribution of one-dimensional peculiar velocities for different cluster masses. Do the clusters exhibit a Gaussian distribution of peculiar velocities? In addition to studying cluster velocities at the present time, we also study how cluster velocities evolve from some early time to the present.

This paper is organized as follows. In Section 2 we describe the algorithms that have been used to identify clusters and to determine their masses and velocities. In Section 3 we study the rms peculiar velocity of clusters for different cluster masses and compare the results with  $\sigma_p(R)$  at different radii. The velocity distribution function is analyzed in Section 4. In Section 5 we briefly discuss the evolution of cluster velocities. A summary and discussion are presented in Section 6.

## 2 SIMULATION OF CLUSTERS

We study cluster velocities in a N-body simulation carried out by the Virgo consortium for the flat  $\Lambda$ CDM model with a cosmological constant. These simulations are described in detail by Jenkins et al. (1998). The simulations were created using an adaptive particle-particle/particle-mesh (AP<sup>3</sup>M) code as described by Couchman, Thomas & Pearce (1995) and Pearce & Couchman (1997). In the  $\Omega_m = 0.3$   $\Lambda$ CDM model studied here, the power spectrum of the initial conditions was chosen to be in the form given by Bond & Efstathiou (1984),

$$P(k) = \frac{Ak}{[1 + (aq + (bq)^{3/2} + (cq)^2)^\nu]^{2/\nu}}, \quad (5)$$

where  $q = k/\Gamma$ ,  $a = 6.4h^{-1}$  Mpc,  $b = 3h^{-1}$  Mpc,  $c = 1.7h^{-1}$  Mpc,  $\nu = 1.13$  and  $\Gamma = \Omega_0 h = 0.21$ . The normalization constant,  $A$ , was chosen by fixing the value of  $\sigma_8$  (the linearly extrapolated mass fluctuation in spheres of radius  $8h^{-1}$  Mpc) to be 0.9. The initial density fluctuation field was assumed to be Gaussian.

The evolution of particles was followed in the comoving box of size  $L = 239.5h^{-1}$  Mpc. The number of particles was  $N_p = 256^3$ . Therefore, the mean particle separation  $\lambda_p = L/N_p^{1/3} = 0.9355h^{-1}$  Mpc and the mass of a particle  $m_p = \rho_b \lambda_p^3 = 6.82 \times 10^{10} h^{-1} M_\odot$ . In the flat  $\Omega_m = 0.3$  model, the dimensionless growth rate  $f = 0.513$  (Peebles 1984).

We used two different algorithms to identify clusters in simulation: the standard friends-of-friends (FOF) algorithm, and the algorithm, where clusters are defined as maxima of the smoothed density field (DMAX).

The friends-of-friends group finder algorithm was applied using the program suite developed by the cosmology group in the University of Washington. These programs are available at <http://www-hpcc.astro.washington.edu>. To test our FOF output data, Suhhonenko & Gramann (2003) investigated the mass function of clusters. The cluster mass function in the Virgo simulations has been studied in detail by Jenkins et al. (2001). Suhhonenko & Gramann (2003) found that the agreement between our results and these obtained by Jenkins et al. (2001) is very good.

The FOF cluster finder depends on one parameter  $b$ , which defines the linking length as  $b\lambda_p$ . The conventional choice for this parameter is  $b = 0.2$  (see e.g. Götz, Huchra & Brandenberger 1998; Jenkins et al. 2001). In this paper we also define clusters by using the value  $b = 0.2$ . We also study velocities of the clusters defined by the parameters  $b = 0.15$ . In the limit of very large numbers of particles per object, FOF approximately selects the matter enclosed by an isodensity contour at  $\rho_b/b^3$ .

We studied FOF clusters that contained at least ten particles. The three-dimensional peculiar velocity of each cluster was defined as

$$\vec{v}_{cl} = \frac{1}{N_f} \sum_{i=1}^{N_f} \vec{v}_i, \quad (6)$$

where  $N_f$  is the number of particles in the cluster and  $\vec{v}_i$  is the peculiar velocity of the particle  $i$  in the cluster.

We also selected DMAX clusters using the following method.

(1) We calculated the density contrast on a grid. For each grid point, the density contrast was determined as

$$\delta = \frac{N}{\bar{N}} - 1, \quad (7)$$

where  $N$  is the number of particles in the sphere of radius  $R_s$  around the grid point, and

$$\bar{N} = \frac{4\pi}{3} \frac{N_p R_s^3}{L^3} \quad (8)$$

is the mean number of particles in the sphere of radius  $R_s$ .

(2) We found the density maxima on the grid. The grid point was considered as a density maximum, if its density contrast was higher than the density contrast in all 26 neighbouring grid points. The location of the grid point, where the density contrast had a maximum value, was identified as the candidate cluster centre.

(3) The final cluster list was obtained by deleting the candidate clusters with lower density contrast in all pairs separated by less than the radius  $R_s$ .

In this way we define the clusters as maxima of the density field smoothed by a top-hat window with a radius  $R_s$ . The smoothing length sets a lower limit on the size of detected structures in the simulations.

We used the smoothing radii  $R_s = 1.5h^{-1}$  Mpc and  $R_s = 1.0h^{-1}$  Mpc. The mean number of particles in spheres of  $R_s = 1.5h^{-1}$  Mpc and  $R_s = 1.0h^{-1}$  Mpc is  $\bar{N} = 17.26$  and  $\bar{N} = 5.12$ , respectively. To select the  $R_s = 1.5h^{-1}$  Mpc clusters, we used a  $256^3$  grid (the cell size  $l = 0.936h^{-1}$  Mpc). For  $R_s = 1.0h^{-1}$  Mpc, we used a  $350^3$  grid ( $l = 0.684h^{-1}$  Mpc). For comparison, for the  $R_s = 1.0h^{-1}$  Mpc clusters we used also a  $256^3$  grid.

We studied the rms density contrast and the rms peculiar velocity on the  $256^3$  grid. The rms density contrast on the grid was 5.05 and 7.29 for the radii  $R_s = 1.5h^{-1}$  Mpc and  $R_s = 1.0h^{-1}$  Mpc, respectively. The rms peculiar velocity,  $\sigma_v$ , was determined for the fraction of grid points,  $F$ , where the number of particles  $N > 1$ . If there are no particles in the neighbourhood of a grid point, the velocity field is undetermined. For  $R_s = 1.5h^{-1}$  Mpc, we found that  $F = 0.96$  and  $\sigma_v = 473 \text{ km s}^{-1}$ . For  $R_s = 1.0h^{-1}$  Mpc,  $F = 0.69$  and  $\sigma_v = 481 \text{ km s}^{-1}$ , respectively. Here we took into account the finite size of the simulation box (see next section). We also studied the rms density contrast and the rms peculiar velocity on the  $350^3$  grid and found similar results.

For each DMAX cluster, we investigated the cluster mass,  $M$ , and the peculiar velocity,  $v_{cl}$ , at the radius  $R_s$ . The mass in the cluster was determined as  $M = N_d m_p$ , where  $N_d$  is the number of particles in a sphere of radius  $R_s$  around the centre of the cluster. The peculiar velocity of each cluster was defined as

$$\vec{v}_{cl} = \frac{1}{N_d} \sum_{i=1}^{N_d} \vec{v}_i, \quad (9)$$

where  $\vec{v}_i$  is the peculiar velocity of the particle  $i$  in the DMAX cluster.

Suhhonenko & Gramann (2003) compared the cluster peculiar velocities defined by different methods (i.e. the FOF method versus the DMAX method) for massive clusters. By using different methods to identify the clusters, we select almost the same objects in the simulation. But we assign different velocities to the same clusters.

### 3 THE RMS PECULIAR VELOCITY OF CLUSTERS

To determine the rms peculiar velocities of clusters, we used the equation

$$v_{rms}^2 = v_s^2 + v_L^2 = \frac{1}{N_{cl}} \sum_{i=1}^{N_{cl}} v_{cli}^2 + v_L^2, \quad (10)$$

where the parameter  $v_s$  describes the dispersion of cluster velocities,  $v_{cli}$ , derived from the simulations and the parameter  $v_L$  is the linear contribution from the velocity fluctuations on scales greater than the size of the simulation box  $L$ . It is given by

$$v_L^2 = \frac{H_0^2 f^2}{2\pi^2} \int_0^{\frac{2\pi}{L}} P(k) dk. \quad (11)$$

$N_{cl}$  is the number of clusters studied. Using eq. (4), the linear rms peculiar velocity of peaks can be written as

$$\sigma_p^2(R) = \sigma_v^2(R) - H_0^2 f^2 \frac{\sigma_0^4(R)}{\sigma_1^2(R)}. \quad (12)$$

The second term in this expression is not sensitive to the amplitude of large-scale fluctuations at wavenumbers  $k < 2\pi/L$ . Therefore, the linear rms velocity of peaks can be expressed, approximately, as

$$\sigma_p^2(R) \approx \sigma_p'^2(R) + v_L^2, \quad (13)$$

**Table 1.** The number of clusters,  $N_{cl}$ , in different mass intervals.

$M$ ( $h^{-1}M_{\odot}$ )	DMAX $R_s = 1.5$	DMAX $R_s = 1.0$	FOF $b=0.2$	FOF $b=0.15$
$10^{12} - 5 \times 10^{12}$	—	70153	51841	47056
$5 \times 10^{12} - 10^{13}$	10647	9989	7326	6764
$10^{13} - 5 \times 10^{13}$	10049	8866	6542	5720
$5 \times 10^{13} - 10^{14}$	1261	1052	856	695
$10^{14} - 5 \times 10^{14}$	688	470	511	393
$5 \times 10^{14} - 10^{15}$	23	4	38	24

where  $\sigma'_p(R)$  is determined by the power spectrum at the wavenumbers  $k > 2\pi/L$  and  $v_L$  is given by eq. (11). For the  $\Lambda$ CDM model studied here, we found that  $v_L = 220 \text{ km s}^{-1}$ .

As a first step, the one-dimensional distribution of cluster velocities can be approximated as a Gaussian distribution (see next section for the study of the velocity distribution of clusters). If the one-dimensional velocities of clusters,  $v_{xi}$ , follow a Gaussian distribution with a mean  $\bar{v}_x = 0$  and a dispersion  $\sigma^2$ , then the sum

$$\chi^2 = \frac{1}{\sigma^2} \sum_{i=1}^{N_{cl}} v_{cli}^2 \quad (14)$$

is distributed as a  $\chi^2$  distribution with the number of degrees of freedom  $\nu = 3N_{cl}$ . In this case, the rms error for the variable  $v_{rms}^2$  can be determined as

$$\Delta v_{rms}^2 = \sqrt{\frac{2}{3N_{cl}}} v_s^2. \quad (15)$$

We used eq. (15) to estimate the error bars for the rms velocities of clusters.

The clusters were divided into subgroups according to their mass. We studied the rms peculiar velocity of clusters in subgroups for which the mass was in the ranges  $(10^{12} - 5 \times 10^{12})h^{-1}M_{\odot}$ , ...,  $(5 \times 10^{14} - 10^{15})h^{-1}M_{\odot}$ . For the DMAX clusters defined with  $R_s = 1.5h^{-1} \text{ Mpc}$ , we considered the clusters with masses  $M > 5 \times 10^{12}h^{-1}M_{\odot}$  ( $N/\bar{N} > 4.24$ ). Table 1 shows the number of clusters and Fig. 1 demonstrates the rms peculiar velocity of clusters in different mass intervals. The rms velocities are shown for the intervals for which the numbers of clusters are  $N_{cl} > 10$ .

Fig. 1a and Fig 1b demonstrate the rms peculiar velocities for the DMAX clusters. Fig. 1a shows the results for the radius  $R_s = 1.5h^{-1} \text{ Mpc}$  and Fig. 1b for the radius  $R_s = 1.0h^{-1} \text{ Mpc}$ . We see that the rms velocity of DMAX clusters is almost independent of the cluster mass. The rms velocity of clusters somewhat increases as the cluster mass increases. However, this increase is small ( $\approx 7$  per cent). For a given scale  $R_s$ , the rms velocity of clusters is similar to the rms velocity for the full grid. The rms velocity of  $R_s = 1.5h^{-1} \text{ Mpc}$  clusters is  $471 \text{ km s}^{-1}$  in the mass interval  $(5 \times 10^{12} - 10^{13})h^{-1}M_{\odot}$  and  $507 \text{ km s}^{-1}$  in the mass interval  $(5 \times 10^{14} - 10^{15})h^{-1}M_{\odot}$ . The rms velocity of  $R_s = 1.0h^{-1} \text{ Mpc}$  clusters is  $495 \text{ km s}^{-1}$  in the mass interval  $(5 \times 10^{12} - 10^{13})h^{-1}M_{\odot}$  and  $510 \text{ km s}^{-1}$  in the mass interval  $(10^{14} - 5 \times 10^{14})h^{-1}M_{\odot}$ . The rms velocities for the  $R_s = 1.5h^{-1} \text{ Mpc}$  clusters are smaller than the rms velocities for the  $R_s = 1.0h^{-1} \text{ Mpc}$  clusters.

The open circles in Fig 1b show the results for the clusters defined by using the  $350^3$  grid. For comparison, we plot-

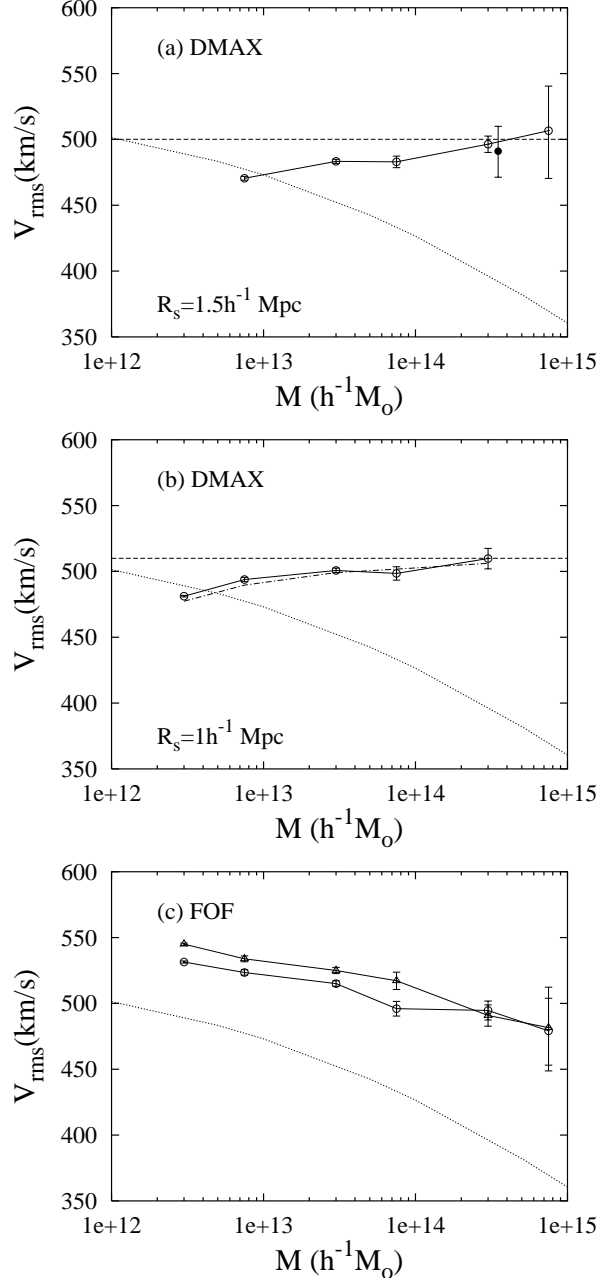


**Figure 1.** The rms peculiar velocities of clusters for different cluster masses. (a) The velocities for the DMAX clusters defined with  $R_s = 1.5h^{-1} \text{ Mpc}$  (open circles). The solid circle represents the result obtained by Colberg et al. (2000). The dashed line shows the linear rms peculiar velocity of peaks,  $\sigma_p$ , for the radius  $R = 1.5h^{-1} \text{ Mpc}$ . (b) The velocities for the  $R_s = 1.0h^{-1} \text{ Mpc}$  DMAX clusters. The circles show the velocities for the clusters defined using a  $350^3$  grid. The dot-dashed line describes the cluster velocities for a  $256^3$  grid. For comparison, we show the linear rms peculiar velocity of peaks for the radius  $R = 1.0h^{-1} \text{ Mpc}$  (dashed line). (c) The velocities of the FOF clusters determined by  $b = 0.2$  (circles) and  $b = 0.15$  (triangles). The dotted line in each panel shows the linear rms peculiar velocity of peaks for the radius  $R = R_L(M)$ .

ted also the rms velocities for the clusters defined by using the  $256^3$  grid. We see that the rms peculiar velocities of clusters in different mass intervals are not sensitive to the number of cells in the grid that was used to find the cluster centres.

Our results are in good agreement with the results obtained Colberg et al. (2000). They also studied the rms velocity of clusters in the  $\Lambda$ CDM model, but used a slightly different method to select clusters. High-density regions were located using a FOF method with  $b = 0.05$  and their barycentres were considered as candidate cluster centers. Any candidate centre for which mass within  $1.5h^{-1}$  Mpc exceeded the threshold mass  $M_t$  was identified as a candidate cluster. The final cluster list was obtained by deleting the lower mass candidate in all pairs separated by less than  $1.5h^{-1}$  Mpc. The peculiar velocity of each cluster was defined to be the mean peculiar velocity of all the particles within the  $1.5h^{-1}$  Mpc sphere. This method to determine the cluster velocities is similar to the DMAX method, if we use the radius  $R_s = 1.5h^{-1}$  Mpc.

In Fig. 1a we show the result obtained by Colberg et al. (2000) for the  $\Lambda$ CDM model. They used the value  $M_t = 3.5 \times 10^{14}h^{-1}M_\odot$ . For this value, the number of clusters was  $N_{cl} = 69$ . They found that the rms cluster velocity derived from simulation is  $v_s = 439 \text{ km s}^{-1}$ . If we include the dispersion  $v_L^2$ , we find that this value of  $v_s$  corresponds to the rms velocity  $v_{rms} = 491 \text{ km s}^{-1}$ . For comparison, we also studied the  $R_s = 1.5h^{-1}$  Mpc clusters with masses  $M > 3.5 \times 10^{14}h^{-1}M_\odot$ . We found 72 clusters with the rms velocity  $v_{rms} = 482_{-19}^{+18} \text{ km s}^{-1}$ . This value is in good agreement with the rms velocity found by Colberg et al. (2000).

For comparison, we show in Fig. 1a and Fig. 1b the rms peculiar velocity of peaks,  $\sigma_p(R)$ , for the radius  $R = R_s$ . For the radii  $R = 1.5h^{-1}$  Mpc and  $R = 1.0h^{-1}$  Mpc, the  $\sigma_p = 500 \text{ km s}^{-1}$  and  $\sigma_p = 510 \text{ km s}^{-1}$ , respectively. We see that the rms velocity of DMAX clusters is well approximated by the linear rms velocity smoothed at the radius  $R = R_s$  (i.e. at the radius which is used to define the cluster velocity). The rms velocity of low-mass clusters is somewhat smaller than predicted by the linear theory.

In Fig. 1c we show the rms peculiar velocities of FOF clusters determined by  $b = 0.2$  and  $b = 0.15$ . The rms velocity of FOF clusters decreases, as the mass of the clusters increases. This result is in agreement with the results obtained by Sheth & Diaferio (2001) and Hamana et al. (2003). They studied the rms velocities of FOF clusters in different mass intervals and found that the rms cluster velocity decreases with mass. Suhhonenko & Gramann (2003) studied the velocities of FOF clusters for different masses and radii. They showed that the effect of the cluster radius on  $v_{rms}$  is similar to the effect of the cluster mass on  $v_{rms}$ . The rms velocity of small FOF clusters is higher than the rms velocity of large massive clusters.

We also plot the linear theory rms peculiar velocity of peaks,  $\sigma_p$ , defined by the linear radius  $R = R_L$  (dotted lines in Fig. 1). In this approximation, the rms peculiar velocity decreases as the cluster mass increases. For the mass  $M = 10^{14}h^{-1}M_\odot$ , the linear radius  $R_L = 6.59h^{-1}$  Mpc and the rms velocity  $\sigma_p(R_L) = 427 \text{ km s}^{-1}$ . For  $M = 5 \times 10^{14}h^{-1}M_\odot$ , we find that  $R_L = 11.3h^{-1}$  Mpc and  $\sigma_p(R_L) = 382 \text{ km s}^{-1}$ . These values for the rms velocities are significantly lower than the rms velocities of clusters

found from the simulation. This result was first obtained by Colberg et al. (2000), who compared the cluster velocities with the linear rms velocities of peaks at the radius  $R = R_L$ .

## 4 VELOCITY DISTRIBUTION FOR THE CLUSTERS

Fig.2 and Fig.3 show the velocity distribution function for the DMAX clusters. We investigated the distribution of one-dimensional cluster peculiar velocities,  $(v_x, v_y, v_z)$ , for different cluster masses. Fig.2 shows the results for the radius  $R_s = 1.5h^{-1}$  Mpc and Fig.3 for the radius  $R_s = 1.0h^{-1}$  Mpc. The probability density was estimated as the normalized number of clusters in the range  $v_1 \pm \Delta v_1$ , as a function of  $v_1$ . We used the value  $\Delta v_1 = 100 \text{ km s}^{-1}$ . We also show the Poisson error bars for the velocity distribution.

We examined the velocity distribution for the clusters in three different mass intervals: (1)  $M = (5 \times 10^{12} - 10^{13})h^{-1}M_\odot$  (Fig. 2a and Fig. 3a), (2)  $M = (10^{13} - 5 \times 10^{14})h^{-1}M_\odot$  (Fig. 2b and Fig. 3b) and (3)  $M > 10^{13}h^{-1}M_\odot$  (Fig. 2c and Fig. 3c). The number of clusters,  $N_{cl}$ , in the mass intervals (1) and (2) is shown in the Table 1. The number of clusters with masses  $M > 10^{13}h^{-1}M_\odot$  is  $N_{cl} = 1973$  and  $N_{cl} = 1526$  for the radius  $R_s = 1.5h^{-1}$  Mpc and  $R_s = 1.0h^{-1}$  Mpc, respectively. We see that the velocity distribution function for different mass intervals is similar.

For comparison, we plot in Fig.2 the Gaussian distribution with the dispersion  $\sigma_1^2$  given by  $\sigma_1 = \sigma'_p/\sqrt{3} = 260 \text{ km s}^{-1}$ . This dispersion is predicted by the linear theory for the scale  $R = 1.5h^{-1}$  Mpc, after accounting for the finite size of the simulation box (see eq. 13). At the radius  $R = 1.5h^{-1}$  Mpc, the rms velocity of peaks  $\sigma_p = 500 \text{ km s}^{-1}$  and, therefore, the parameter  $\sigma'_p = 450 \text{ km s}^{-1}$ . Fig. 2 demonstrates that the one-dimensional velocity distribution function for  $R_s = 1.5h^{-1}$  Mpc clusters is well approximated by a Gaussian.

In Fig.3 we compare the velocity distribution of  $R_s = 1.0h^{-1}$  Mpc clusters with the Gaussian distribution for  $\sigma_1 = 265 \text{ km s}^{-1}$ . At the radius  $R = 1.0h^{-1}$  Mpc, the rms velocity of peaks  $\sigma_p = 510 \text{ km s}^{-1}$  and, therefore,  $\sigma'_p = 460 \text{ km s}^{-1}$ . We see that the velocity distribution of  $R_s = 1.0h^{-1}$  Mpc clusters is also similar to the Gaussian distribution. However, there are small deviations from the Gaussian distribution, especially for the clusters with masses  $M = (10^{13} - 5 \times 10^{13})h^{-1}M_\odot$ .

During the evolution larger and larger scales become non-linear and deviations from the Gaussian distribution develop. As demonstrated by Bachall, Gramann & Cen (1994) and Sheth & Diaferio (2001), evolution of the cluster peculiar velocities depends on the large-scale density field. The highest velocity clusters frequently originate in dense superclusters. Fig. 3 demonstrates how the deviations from the Gaussian distribution start to develop.

Fig. 4 shows the velocity distribution function for the FOF clusters determined by  $b = 0.2$ . We studied also the velocity distribution for the clusters defined by  $b = 0.15$  and found similar results. The velocity distribution was determined in different mass intervals. For comparison, we plot the Gaussian distribution function with the dispersion  $\sigma_x^2$  as determined for the  $v_x$  velocities in the simulation. The

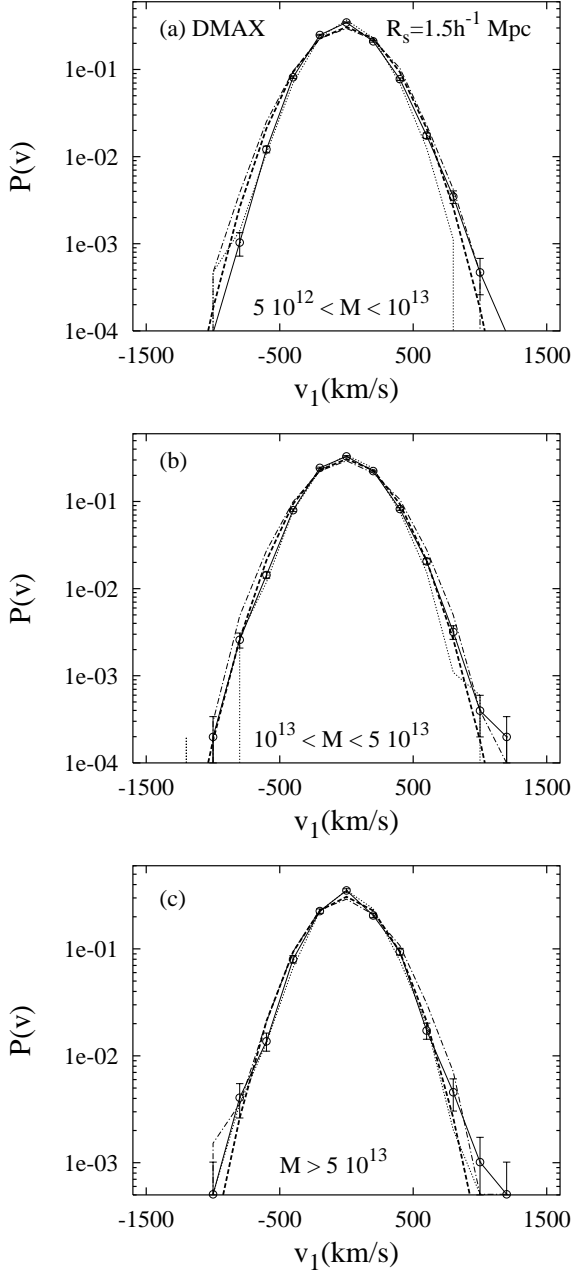


**Figure 2.** Probability densities of one-dimensional cluster velocity  $v_1$  for limited mass ranges (denoted in each panel). Clusters are defined by the DMAX method with the radius  $R_s = 1.5h^{-1}$  Mpc. The solid, dot-dashed and dotted lines show the distribution of the three Cartesian components ( $v_x, v_y, v_z$ ), respectively. For clarity, the error bars are shown only for the  $v_x$  distribution. The heavy dashed line in each panel describes the Gaussian distribution predicted by the linear theory for the scale  $R = 1.5h^{-1}$  Mpc ( $\sigma_1 = 260 \text{ km s}^{-1}$ ).

parameter  $\sigma_x = 266, 264$  and  $246 \text{ km s}^{-1}$  in the Fig. 4a, Fig. 4b and Fig. 4c, respectively.

The velocity distribution of FOF clusters in different mass intervals is different. In Fig 4a and Fig. 4b, we see that the peculiar velocity distributions found for the clusters have stronger peculiar velocity tails than predicted by a Gaussian distribution. Deviations from the Gaussian distribution are

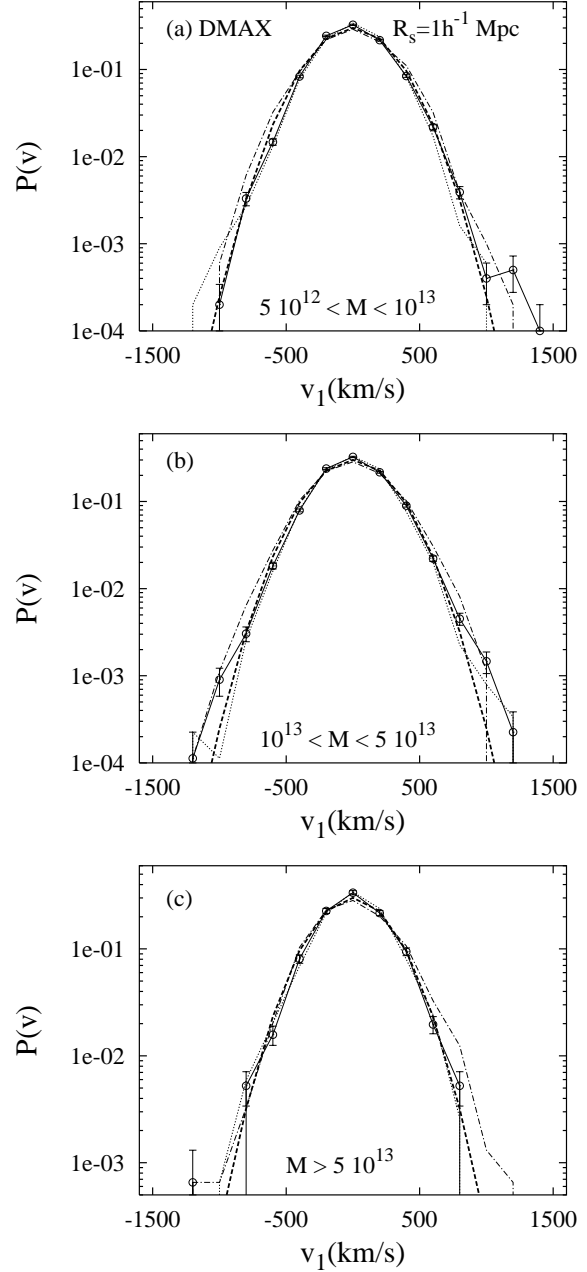


**Figure 3.** As for the previous figure, but for the DMAX clusters defined with the radius  $R_s = 1.0h^{-1}$  Mpc. The heavy dashed line in each panel describes the Gaussian distribution predicted by the linear theory for the scale  $R = 1.0h^{-1}$  Mpc ( $\sigma_1 = 265 \text{ km s}^{-1}$ ).

larger for small low-mass clusters. This result for the FOF clusters was obtained also by Hamana et al. (2003), who studied the velocity distribution for clusters with masses  $M < 3.2 \times 10^{13} h^{-1} M_\odot$  (see Fig. 5 in their study). We also investigated the velocity distribution for massive clusters with  $M > 5 \times 10^{13} h^{-1} M_\odot$  (Fig. 4c). The velocity distribution of massive FOF clusters is similar to the Gaussian distribution.

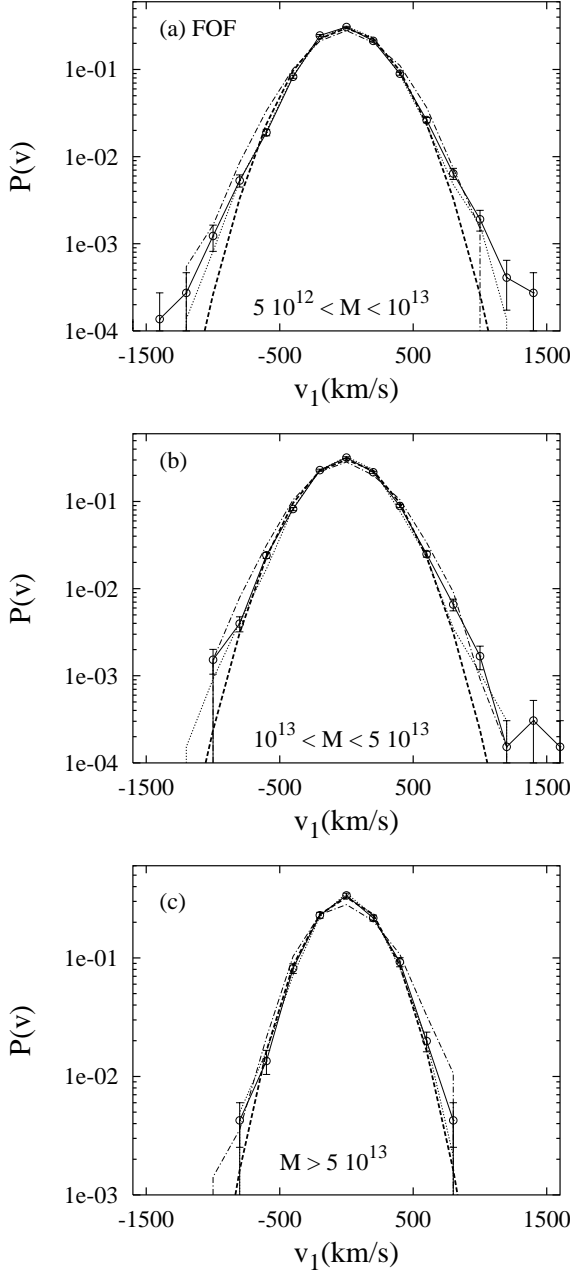


**Figure 4.** As for the figures Fig.2 and Fig.3, but for the FOF clusters determined by  $b = 0.2$ . The heavy dashed line in each panel describes the Gaussian distribution function with the dispersion  $\sigma_x^2$  as computed for the  $v_x$  velocities in the N-body simulation.

## 5 EVOLUTION OF CLUSTER VELOCITIES

We investigated the evolution of cluster velocities by using the Virgo simulation for the  $\Lambda$ CDM model at redshift  $z = 10$ .

We selected 509 clusters with masses  $M > 1.2 \times 10^{14} h^{-1} M_\odot$  at  $z = 0$ . The mean intercluster separation in this sample was  $d_{cl} = 30 h^{-1}$  Mpc. The rms velocity of the clusters was  $v_{rms} = 494 \text{ km s}^{-1}$ . The clusters were determined with the DMAX method, using the radius  $R_s = 1.5 h^{-1}$  Mpc. For each cluster, we found all particles within a  $1.5 h^{-1}$  Mpc sphere around the centre of the cluster

and determined the positions of these particles at  $z = 10$ . We define the initial centre of the cluster at  $z = 10$  to be the barycentre of these particles.

Are these initial centres of the clusters associated with peaks in the density field at  $z = 10$ ? We studied the density field in the Virgo simulation at  $z = 10$ . To identify the peaks in the density field, we used the DMAX method with the radius  $R_s = 1.5 h^{-1}$  Mpc (comoving). The rms density contrast on the  $256^3$  grid was  $\sigma_0 = 0.31$ . For each peak, we determined the dimensionless height of a peak,  $\nu$ , and the peculiar velocity of a peak,  $v_p$ . The parameter  $\nu$  was defined as

$$\nu = \frac{1}{\sigma_0} \left( \frac{N_d}{\bar{N}} - 1 \right), \quad (16)$$

where  $N_d$  was the number of particles in the sphere of radius  $R_s$  around the centre of the peak and  $\bar{N}$  was the mean number of particles in this sphere (see eq. 8). The peculiar velocity of a peak was defined to be the mean velocity of particles in the sphere of radius  $R_s$ . The velocities of the peaks were scaled up to the values expected at  $z = 0$  according to the linear theory. In the linear regime, the peculiar velocity  $v \sim aDHf$ , where  $a$  is the scale factor and  $D$  is the linear growth factor. By taking into account the evolution of these four functions, we found that  $v(z = 0) = 2.42 v(z = 10)$ . In the following we consider only peaks with  $\nu > 3$ . The rms peculiar velocity of these peaks was  $516 \text{ km s}^{-1}$  (scaled up to  $z = 0$ ).

We investigated the peaks within a  $3.0 h^{-1}$  Mpc sphere around the initial centre of the clusters. We found that 413 clusters (81 per cent) are associated with a peak or peaks in the density field at  $z = 10$ . Most of the remaining clusters can be associated with a peak of either a slightly lower height or at a slightly greater separation. For 205 clusters, we found one peak at the initial centre of the cluster. 144 clusters were associated with two peaks. For 64 clusters, we found three or more peaks.

In Fig. 5 we compare the peculiar velocities of peaks at the initial centres of clusters with the final peculiar velocities of clusters at  $z = 0$ . In Fig. 5a we show the velocities for the clusters associated with one peak. Fig. 5b describes the results for the clusters associated with two peaks. We see the correlation between the peculiar velocities of clusters and their associated peaks. In Fig. 5a, the rms difference in (3-D) peculiar velocity between a cluster and its associated peak is  $246 \text{ km s}^{-1}$ . In Fig. 5b, the rms difference is  $262 \text{ km s}^{-1}$ .

At  $z = 0$ , the density field is highly non-linear at the scale  $R = 1.5 h^{-1}$  Mpc. The rms density contrast is 5.03. We cannot consider the density maxima in this field as separate objects, which move with linear speeds. During the evolution many density maxima merge and lose their identity. Some clusters obtain higher velocities than the values expected according to the linear scaling, other clusters move at lower velocities. However, these effects compensate each other. Our results show that the rms peculiar velocity of density maxima at  $z = 0$  is well approximated by the linear rms velocity expected on a given scale. The rms peculiar velocity of density maxima is similar to the rms peculiar velocity for all field points at the same scale. In other words, the rms peculiar velocity does not depend much on the location of spheres used to determine the velocities. In comparison with the density field, the velocity field is more heavily weighted

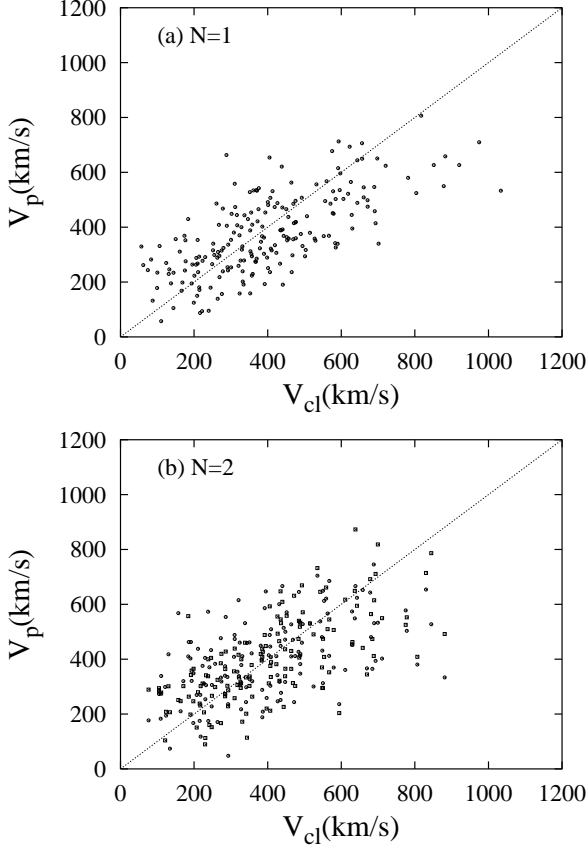


**Figure 5.** Peculiar velocities of peaks at the initial centre of the clusters,  $v_p$ , as compared with the final peculiar velocities of clusters,  $v_{cl}$ , at  $z = 0$ . The velocities of peaks are scaled up to values expected at  $z = 0$  according to the linear theory. (a) Velocities for the 205 clusters associated with one peak. (b) Velocities for the 144 clusters associated with two peaks. Different symbols in the panel (b) show the velocities for the different peaks.

by modes with low values of the wavenumber  $k$ , i.e. large scales which are in the linear regime.

## 6 SUMMARY AND DISCUSSION

In this paper we have examined peculiar velocities of clusters predicted in the  $\Lambda$ CDM model. We analyzed the clusters in the Virgo simulation for the  $\Lambda$ CDM model with  $\Omega_0 = 0.3$ ,  $h = 0.7$  and  $\sigma_8 = 0.9$ . To identify clusters in the simulation we used two methods: (1) the standard friends-of-friends (FOF) method and (2) the method, where the clusters are defined as the maxima of the smoothed density field (DMAX). We used a top-hat window with smoothing radii  $R_s = 1.5h^{-1}$  Mpc and  $R_s = 1.0h^{-1}$  Mpc. The peculiar velocity of DMAX clusters was defined to be the mean peculiar velocity within a sphere of radius  $R_s$ .

We studied the rms peculiar velocity of clusters for different cluster masses. We found that the relation between the rms peculiar velocity of a cluster and the mass of the cluster depends on the method that is used to determine the cluster masses and velocities. The rms peculiar velocity of FOF clusters decreases as the mass of the clusters increases. The rms peculiar velocity of DMAX clusters is

almost independent of the cluster mass and is well approximated by the linear rms velocity of peaks of the density field smoothed at the radius  $R = R_s$ . We also studied the rms peculiar velocities of peaks,  $\sigma_p$ , for the linear smoothing radius  $R = R_L(M)$ . In this approximation, the rms velocities are significantly lower than the rms velocities of clusters found in the simulation.

We investigated the distribution functions of the cluster peculiar velocities for different cluster masses. The peculiar velocity distributions found for the low-mass FOF clusters have stronger tails than predicted by a Gaussian distribution. But the velocity distribution of massive FOF clusters is similar to the Gaussian distribution. The velocity distribution of DMAX clusters in different mass intervals is similar. The one-dimensional velocity distribution of  $R_s = 1.5h^{-1}$  Mpc clusters is well approximated by a Gaussian. In the velocity distribution of  $R_s = 1.0h^{-1}$  Mpc clusters, we found small deviations from the Gaussian distribution.

We also investigated the evolution of cluster velocities on the scale  $R_s = 1.5h^{-1}$  Mpc. We found a correlation between the peculiar velocities of massive clusters at  $z = 0$  and the peculiar velocities of peaks at the initial centres of the clusters at  $z = 10$ . Density maxima at the scale  $R_s = 1.5h^{-1}$  Mpc are not isolated objects that move with linear speeds.

In this paper we introduced the DMAX method. This method operates with the smoothed density and velocity fields on a given scale  $R_s$ . We expect that the properties of DMAX clusters (e.g. their mass distribution, correlation function) can be determined analytically from the properties of initial density and velocity fields, at least, for the quasi-linear scales. The density and velocity distribution function for the maxima in the Gaussian density field was derived by Bardeen et al. (1986). Further study is needed to consider different properties of the DMAX clusters.

We found that the rms velocities of DMAX clusters on a given scale  $R_s$  are well described by the linear theory at  $R = R_s$  (equation 4). Suhhonenko & Gramann (2003) studied the rms peculiar velocities of clusters in the  $\tau$ CDM model. They found that also in this model, the rms peculiar velocities of DMAX clusters are close to the linear theory expectations. We can use the linear approximation to estimate rms peculiar velocities of clusters in different cosmological models.

Fig. 6 shows the rms peculiar velocities of clusters estimated for different  $\Lambda$ CDM models using the approximation (4). Fig. 6a shows the results for the radius  $R = 1.5h^{-1}$  Mpc and Fig. 6b for the radius  $R = 1.0h^{-1}$  Mpc, respectively. We estimated the rms peculiar velocity of clusters in flat  $\Lambda$ CDM models, where the density parameter  $\Omega_m = 0.2-0.35$ , the normalized Hubble constant  $h = 0.65-0.7$  and  $\sigma_8 = 0.7-0.9$ . The power spectrum of density fluctuations was chosen as  $P(k) = AkT^2(k)$ , where the transfer function  $T(k)$  was calculated using the fast Boltzmann code CMBFAST developed by Seljak & Zaldarriaga (1996). The normalization constant,  $A$ , was chosen by fixing the value of  $\sigma_8$ . On large scales, the power spectrum calculated by using the code CMBFAST is higher than the power spectrum given by equation (5) (for a fixed  $\sigma_8$ ; see, e.g., Fig. 2 by Gramann & Suhhonenko 2002). To determine the dimensionless growth rate  $f$ , we used the equations given by Peebles (1984).

Consider the peculiar velocities of clusters for the smoothing radius  $R = 1.5h^{-1}$  Mpc. If  $h = 0.7$  and  $\sigma_8 = 0.7$ ,



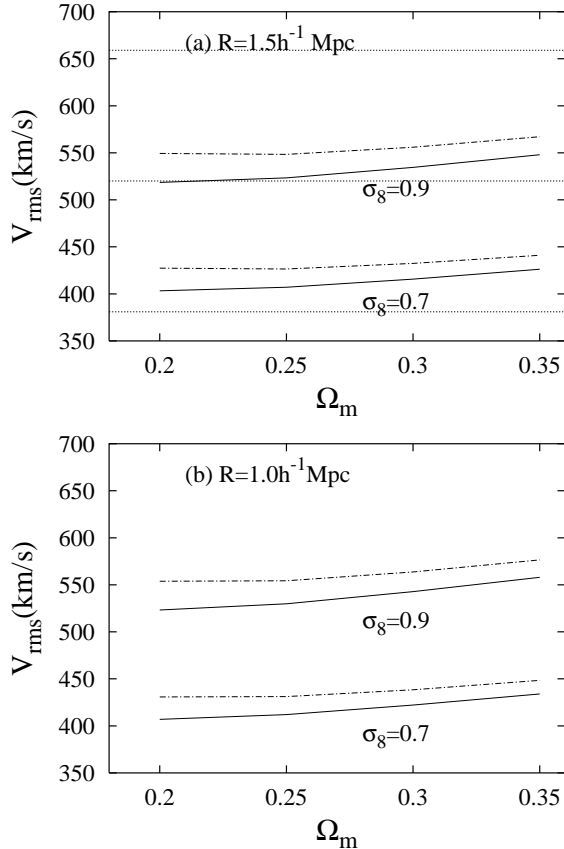


**Figure 6.** The rms peculiar velocities of clusters predicted in different flat  $\Lambda$ CDM models. (a) The peculiar velocities are smoothed on the scale  $R = 1.5h^{-1}$  Mpc. (b) The smoothing radius  $R = 1.0h^{-1}$  Mpc. The solid lines show the results for  $h = 0.7$  and the dot-dashed lines for  $h = 0.65$ . The upper curves describe the velocities for  $\sigma_8 = 0.9$  and lower curves for  $\sigma_8 = 0.7$ . Dotted lines in panel (a) describe the rms peculiar velocity obtained by Giovanelli et al. (1998) for 24 observed clusters. They found that the rms cluster peculiar velocity is  $v_{rms} = 520 \pm 139 \text{ km s}^{-1}$ .

the rms peculiar velocity of clusters is  $403 \text{ km s}^{-1}$  for  $\Omega_m = 0.2$  and  $426 \text{ km s}^{-1}$  for  $\Omega_m = 0.35$ . For a higher density parameter  $\Omega_m$ , the function  $f$  is larger, but the amplitude of the large-scale density fluctuations is smaller. If  $h = 0.7$  and  $\sigma_8 = 0.9$ , the rms peculiar velocity of clusters is  $518 \text{ km s}^{-1}$  and  $548 \text{ km s}^{-1}$  for  $\Omega_m = 0.2$  and  $\Omega_m = 0.35$ , respectively.

For comparison, we show in Fig.6a the rms peculiar velocity obtained by Giovanelli et al. (1998) for 24 observed clusters in the distance range  $\sim 10$  and  $90h^{-1}$  Mpc. This comparison is very preliminary. The peculiar velocities for the observed galaxy clusters and for the simulated DMAX clusters are determined in different ways. Giovanelli et al. (1997) analysed the I-band Tully-Fisher (T-F) measurements for 782 spiral galaxies in the fields of 24 clusters (the SCI sample). Most of the galaxies used in the T-F analysis were within the Abell radius ( $R_A = 1.5h^{-1}$  Mpc) around the cluster centre. The peculiar velocities for the clusters in this sample were studied by Giovanelli et al. (1998). Individual cluster T-F relations were referred to the average template relation to compute cluster peculiar velocities. Giovanelli et al. (1998) found that the rms one-dimensional clus-

ter peculiar velocity in the SCI sample is  $300 \pm 80 \text{ km s}^{-1}$ , which corresponds to the three-dimensional rms velocity  $v_{rms} = 520 \pm 139 \text{ km s}^{-1}$ . This number is in good agreement with previous estimates by Bahcall & Oh (1996) and by Watkins (1997), based on the SCI sample. This estimate is also in agreement with that determined for the SCII sample (Dale et al. 1999b). The SCII sample is based on T-F measurements for 522 late-type galaxies in the fields of 52 Abell clusters in the distance range  $\sim 50$  to  $200h^{-1}$  Mpc. The distribution of these galaxies in the 35 Abell clusters was presented by Dale et al. (1999a). Dale et al. (1999b) studied the cluster peculiar velocities in the SCII sample and found that the rms one-dimensional cluster peculiar velocity in this sample is  $341 \pm 93 \text{ km s}^{-1}$ . This corresponds to the three-dimensional rms velocity  $591 \pm 161 \text{ km s}^{-1}$ .

Yoshikawa, Jing & Börner (2003) analyzed the velocity dispersion of galaxies,  $\sigma_{gal}$ , and of dark matter,  $\sigma_{dm}$ , inside clusters using hydrodynamical simulations. They found that the velocity dispersions of galaxies in less massive ( $\sim 10^{13} M_\odot$ ) clusters are systematically lower than those of dark matter particles inside the clusters. We do not exactly know how the mean peculiar velocity of galaxies is related to the mean velocity of matter in the cluster. It is usually assumed that these velocities are similar. Further work is needed to study the peculiar velocities of galaxy clusters in the hydrodynamical simulations.

## ACKNOWLEDGEMENTS

We thank J. Einasto, M. Einasto, P. Heinämäki, G. Hütsi, E. Saar and S. White for useful discussions. This work has been supported by the ESF grant 5347. The N-body simulations used in this paper are available at <http://www.mpa-garching.mpg.de/Virgo/virgoproject.html>. These simulations were carried out at the Computer Center of the Max-Planck Society in Garching and at the EPCC in Edinburgh, as part of the Virgo Consortium project. The FOF programs used in this paper are available at <http://www-hpcc.astro.washington.edu>. These programs were developed in the University of Washington.

## REFERENCES

- Bahcall N.A., Gramann M., Cen R. 1994, ApJ, 436, 23
- Bahcall N.A., Oh S.P. 1996, ApJ, 462, L49
- Bardeen J.M., Bond J.R., Kaiser N., Szalay A.S. 1986, ApJ, 304, 15
- Brainerd T.G., Villumsen J.V., 1994, ApJ, 436, 528
- Bond J.R., Efstathiou G., 1984, ApJ, 285, L45
- Borgani S., Bernardi M., da Costa L.N., Wegner G., Alonso M.V., Willmer C.N.A., Pellegrini P.S., Maia M.A.G., 2000, ApJ, 537, L1
- Ciecielag P., Chodorowski M.J., Kiraga M., Strauss M.A., Kudlicki A., Bouchet F.R., 2003, MNRAS, 339, 641
- Colberg J.M., White S.D.M., MacFarland T.J., Jenkins A., Pearce F.R., Frenk, C.S., Thomas P.A., Couchman H.M.P., 2000, MNRAS, 313, 229
- Colin, P., Klypin A.A., Kravtsov V., 2000, ApJ, 539, 561
- Croft R.A.C., Efstathiou G., 1994, MNRAS, 268, L23
- Couchman H.M.P., Thomas P.A., Pearce F.R., 1995, ApJ, 452, 797

- Dale D.A., Giovanelli R., Haynes M.P., Hardy E., Campusano L.E., 1999a, AJ, 118, 1468
- Dale D.A., Giovanelli R., Haynes M.P., Campusano L.E., Hardy E., 1999b AJ, 118, 1489
- Davis M., Efstathiou G., Frenk C.S., White S.D.M., 1985, ApJ, 292, 371
- Giovanelli R., Haynes M.P., Herter T., Vogt N.P., Wegner G., Salzer J.J., da Costa L.N., Freudling W., 1997, AJ, 113, 22
- Giovanelli R., Haynes M.P., Salzer J.J., Wegner G., da Costa L.N., Freudling W., 1998, AJ, 116, 2632
- Gramann M., Bahcall N., Cen R., Gott J.R., 1995, ApJ, 441, 449
- Gramann M., Suhhonenko I., 2002, MNRAS, 337, 1417
- Götz M., Huchra J.P., Brandenberger R.H., astro-ph:9811393
- Hamana T., Kayo I., Yoshida N., Suto Y., Jing Y.P., 2003, MNRAS in press, astro-ph: 0305187
- Yoshikawa K., Jing Y.P., Börner G., 2003, MPA preprint
- Jenkins A. et al. (The Virgo Consortium), 1998, ApJ, 499, 20
- Jenkins A., Frenk C.S., White S.D.M., Colberg J.M., Cole S., Evrard A.E., Couchman H.M.P., Yoshida N., 2001, MNRAS, 321, 372
- Juszkiewicz, R., Springel V., Durrer R., 1999, ApJ, 518, L25
- Kofman L., Bertschinger E., Gelb J.M., Nusser A., Dekel A., 1994, ApJ, 420, 44
- Lahav O., Lilje P.B., Primack J.R., Rees M.J., 1991, MNRAS, 251, 128
- Moscardini L., Branchini E., Brunozzi P.T., Borgani S., Plionis M., Coles P. 1996, MNRAS, 282, 384
- Pearce F.R., Couchman H.M.P., 1997, NewA, 2, 411
- Peebles P.J.E., 1984, ApJ, 284, 439
- Sheth R.K., Diaferio A., 2001, MNRAS, 322, 901
- Suhhonenko I., Gramann M., 1999, MNRAS, 303, 77
- Suhhonenko I., Gramann M., 2003, MNRAS, 339, 271
- Watkins R. 1997, MNRAS, 292, L59